RSC Advances

PAPER

View Article Online
View Journal | View Issue



Cite this: *RSC Adv.*, 2023, **13**, 28104

# Janus metallic film with gold and silver luster by electroless deposition of silver using poly(dopamine acrylamide) thin film†

Mizuki Ohke,[a] Ryoichi Akaishi,[b] Kyoka Tachibana,[c] Michinari Kohri,[c] Shusaku Nagano,[d] Hinako Ebe[e] and Jun Matsui *[e]

Received 27th July 2023
Accepted 12th September 2023

DOI: 10.1039/d3ra05099h

rsc.li/rsc-advances

Films that exhibit different metallic luster on the front and back, called Janus metallic films, have broad applications ranging from design materials to optical devices. However, the fabrication of these films is often a complicated process involving multiple metal deposition steps, thermal annealing, and calcination. Herein, we report the simple preparation of a Janus metallic film by electroless deposition of silver on a poly(dopamine acrylamide) (pDOPAm) thin film. pDOPAm was successfully synthesized *via* the controlled reversible addition–fragmentation chain transfer polymerization of dopamine acrylamide without a protective group using dimethylformamide as the solvent. The synthesized pDOPAm was spin-coated onto a solid substrate, which was then immersed in an aqueous $AgNO_3$ solution to achieve the electroless deposition of silver. Our preparation method will considerably simplify the fabrication of Janus metallic films, enabling their widespread application as decorative or authentication materials.



## Introduction

Glass and polymer films with metallic luster are widely used as reflective mirrors, heat-resistant films, and artistic ornaments.[1,2] In particular, films with different metallic luster on the front and back, called Janus metallic films, have not only high design quality but also unique optical applications, such as color routing.[3] To create Janus metallic films, different metals must be deposited on the front and back sides of a substrate. However, this involves complicated and expensive processes owing to the use of at least two metals. Recently, Tatsuma *et al.* reported that sequentially stacked Ag and/or Au nanoparticles (NPs) of different sizes exhibit different colors on the front and back depending on the incidence angle of light.[4,5] The Janus-like coloring was attributed to the combination of plasmon resonance and difference in the reflective index gradient between the incident light from the front (Au NPs/Ag NPs/$SiO_2$/$TiO_2$/glass) and back sides (glass/$TiO_2$/$SiO_2$/Ag NPs/Au NPs). Although metal NPs are useful for fabricating Janus metallic films, they entail multiple deposition processes, thermal annealing, and calcination.[4–6] To date, the use of a single metallic element to fabricate Janus metallic films has not been reported.

Metal NPs are generally synthesized *via* the chemical reduction of metal salts. However, catechol has been increasingly used as a reducing agent to produce metal NPs. This multifunctional molecule is responsible for the adhesive properties of the byssal plaque of marine organisms such as mussels. Catechol with 1,2-dihydroxy groups adheres to several surfaces, from hydrophilic $TiO_2$ to hydrophobic polytetrafluoroethylene.[7–11] Yabu *et al.* combined the strong adhesive and reductive properties of catechol to produce a well-aligned NP film using a block copolymer containing a catechol moiety.[12] Zhang *et al.* coated the inner wall of a glass microchannel with a catechol polymer to enable the deposition of Ag nanocatalysts.[13] Singer *et al.* inkjet-printed catechol NPs onto a substrate and electroless-plated Ag to produce metal line patterns.[14]

In the present study, we developed a facile fabrication method for Janus metallic films using a single metallic element and the cathecol-based polymer poly(dopamine acrylamide) (pDOPAm). Electroless plating of Ag on a pDOPAm thin film resulted in a Janus metallic film that showed gold and silver luster on the front and back, respectively. The metallic luster of the Janus metallic film was characterized by ultraviolet-visible (UV-vis) reflectance spectroscopy. Furthermore, the surface and cross-sectional structures of the Janus metallic film were

[a]*Graduate School of Science and Engineering, Yamagata University, 1-4-12 Kojirakawa-machi, Yamagata 990-8560, Japan*
[b]*Osaka Organic Chemical Industry Ltd., 18-8 Katayama-cho, Kashiwara City, Osaka 582-0020, Japan*
[c]*Graduate School of Engineering, Chiba University, 1-33 Yayoicho, Inage-ku, Chiba 263-8522, Japan*
[d]*College of Science, Rikkyo University, 3-34-1 Nishi-Ikebukuro, Toshima-ku, Tokyo 171-8501, Japan*
[e]*Faculty of Science, Yamagata University, 1-4-12 Kojirakawa-machi, Yamagata 990-8560, Japan. E-mail: jun_m@sci.kj.yamagata-u.ac.jp*

† Electronic supplementary information (ESI) available. See DOI: https://doi.org/10.1039/d3ra05099h

observed by scanning electron microscopy (SEM) to investigate its coloration mechanism.

## Experimental section

### Materials

2,2′-Azobis(isobutyronitrile) (AIBN, FUJIFILM Wako) was recrystallized from ethanol. Dopamine acrylamide (DOPAm, Osaka Organic Chemical Industry Ltd.), *N*,*N*-dimethylformamide (DMF, dehydrated, Kanto Chemical), acetone (Nacalai Tesque), isopropyl alcohol (Nacalai Tesque), diethyl ether (Nacalai Tesque), and silver nitrate (Kanto Chemical) were used as received.

### Equipment

The structure of pDOPAm was characterized by $^1$H NMR spectroscopy (ECA-500, JEOL) in DMSO-$d_6$. The number-average molecular weight ($M_n$) and molecular weight dispersity ($M_w$/$M_n$) of pDOPAm were measured by gel permeation chromatography (GPC; HLC-8320GPC, Tosoh Techno-System, Inc. and LC-10ADVP, Shimadzu Corp.) using polystyrene standards and DMF as the eluent at 40 °C. The thermophysical properties of pDOPAm were measured by differential scanning calorimetry (DSC; DSC8231, Rigaku Corp.) under $N_2$ flow (50 mL min$^{-1}$) at a heating rate of 10 °C min$^{-1}$ in the temperature range of −40–150 °C. The spectra of Ag and Au were obtained by UV-vis transmission (UV-3150, Shimadzu Corp.) and reflectance spectroscopy (MSV-370, Jasco) using an Ag plate (Nilaco Corp.) and Au foil (Hakuichi) as references, respectively. The surface morphology of the pDOPAm thin film was examined by SEM (JSM-7600F, JEOL) at an acceleration voltage of 5 kV. Cross-sectional observation and elemental analysis of the pDOPAm thin film were performed by SEM with energy-dispersive X-ray spectroscopy (SEM-EDS). Cyclic voltammetry (ECstat-400, EC FRONTIER) was used to probe the electrochemistry of pDOPAm.

### Synthesis of pDOPAm

pDOPAm was synthesized *via* reversible addition–fragmentation chain transfer (RAFT) polymerization using AIBN as the thermal initiator and 2-cyano-2-propyl dodecyl trithiocarbonate (CTA) as the chain-transfer agent (Scheme 1). DOPAm (1.50 g), AIBN ($5.94 \times 10^{-3}$ g), and CTA ($2.50 \times 10^{-2}$ g) were added to a pressure-resistant glass tube (Ace Glass). DMF (1.0 M) was added to this glass tube in a glove box filled with $N_2$. The reaction was conducted for a predetermined time and terminated by exposure to air. To collect pDOPAm, most of the DMF was evaporated under reduced pressure, and the solution was dropped into a large quantity of diethyl ether to precipitate pDOPAm. The obtained pDOPAm was dissolved in DMF and reprecipitated twice from diethyl ether. Finally, pDOPAm was collected and dried at room temperature under reduced pressure.

### Thin-film preparation

Silicon (Si), glass, and quartz substrates were ultrasonically cleaned in acetone and then continuously cleaned in isopropyl alcohol for 20 min. This cleaning procedure was repeated twice before treating the substrate surfaces with UV-$O_3$ (PL16-110, SEN Lights Corp). Before use, the hydrophilic substrates were dried under $N_2$ flow. Thin films were prepared by spin-coating (MA-A100, Mikasa) a 5 wt% pDOPAm/DMF solution onto each substrate. The substrates were centrifuged at 1000 rpm for 10 s, 1500 rpm for 120 s, and 2500 rpm for 30 s. The prepared films were annealed at 90 °C for 2 h under a pressure of less than 0.1 kPa in a vacuum drying oven (ADP220, Yamato Kagaku) to remove any residual solvent.

### Electroless deposition of silver on the thin films

A solid substrate coated with a pDOPAm film was immersed in aqueous $AgNO_3$ (200 mM) in a Petri dish (Fig. S1†). The Petri dish was then placed in a sealed container with six vials, each containing 10 mL distilled water. The container was sealed and heated for a specific duration at a specific temperature.

### Cyclic voltammetry of pDOPAm[15]

Voltammogram was acquired in 3-electrode cells in aqueous. Glassy carbon was used as the working electrode and Pt electrode as the counter electrode. Ag/AgCl was used as the reference electrode. The aqueous electrolyte was a 0.1 M phosphate buffer at pH = 8. The polymer samples were dissolved in the electrolyte at a concentration of 1 mM. This voltammograms was taken at a scan rate of 100 mV s$^{-1}$.

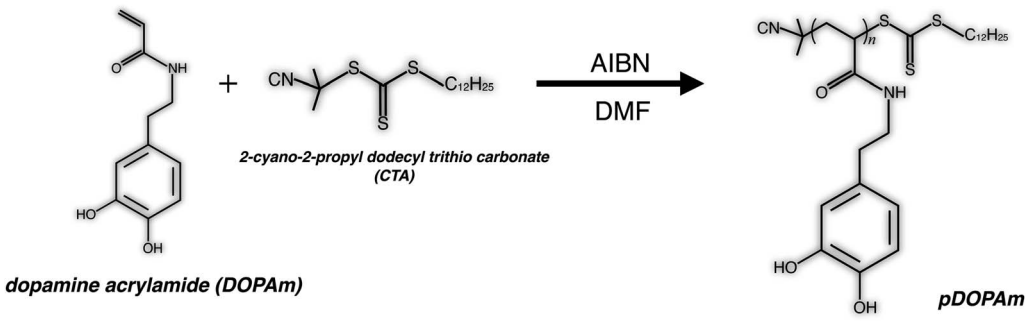


Scheme 1 Synthesis of poly(dopamine acrylamide) (pDOPAm).

## Results and discussion

### Characterization of pDOPAm

pDOPAm was synthesized *via* the RAFT polymerization of DOPAm (Scheme 1). The process was monitored by $^1$H NMR spectroscopy (Fig. S2†) and GPC (Fig. 1A and B). $M_n$ remained at 5400 despite the consumption of the monomers after 60 min of polymerization. Subsequently, pseudo-first-order kinetic plot as a function of time shows that the semilogarithmic plot was linear with respect to time above 120 min (Fig. 1A). Moreover, $M_n$ was linearly increased with respect to conversion of DOPAm while $M_w/M_n$ remained below 1.4 (Fig. 1B). The near-linear increase in $M_n$ with polymerization time and the low $M_w/M_n$ indicate that the RAFT polymerization of DOPAm was well controlled after 120 min of polymerization, resulting in a narrower $M_w/M_n$ compared with that for the free radical polymerization of DOPAm (Fig. S3A and B†). We considered that the bimolecular reaction between DOPAm monomers predominated at less than 120 min of polymerization owing to the low RAFT agent concentration. A previous study indicated that catechol OH groups are protected by hydrogen bonding with DMF.[16] We believe this "on-demand protection" enables control of the RAFT polymerization of unprotected DOPAm. Subsequently, the polymer obtained after 360 min was purified by reprecipitation and characterized by $^1$H NMR spectroscopy. The peak of the vinyl group (5.5–6.3 ppm) disappeared, while the peaks of the polymer main chain (~2.5 ppm), aromatic group (6.2–6.8 ppm), and hydroxyl groups (8.5–9.0 ppm) were detected. Moreover, the peaks of the dodecyl side chain (1.1–1.3 ppm) and methyl group in CTA (0.8–0.9 ppm) were observed (Fig. S2†). The UV-vis spectrum of pDOPAm exhibited an absorption peak originating from the catechol groups at $\lambda$ = 290 nm (Fig. 2).[17] Notably, no absorption was observed at neither $\lambda \approx 340$ nm, which originates from bimolecular cross-linked catechol, nor $\lambda$ = 390–395 nm, which is associated with a catechol with a quinone structure.[17,18] Thus, the obtained pDOPAm did not contain any oxidized forms of catechol. The thermophysical properties of the synthesized pDOPAm were investigated by DSC. pDOPAm showed a baseline shift at ~60 °C, which was assigned to the glass transition temperature ($T_g$ = 66.4 °C) (Fig. 3). This result is similar to a previously reported value ($T_g \approx$ 69 °C).[17]

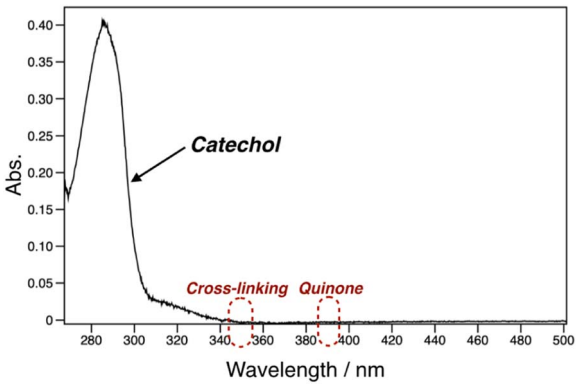


Fig. 2 UV-vis spectrum of poly(dopamine acrylamide) (pDOPAm).

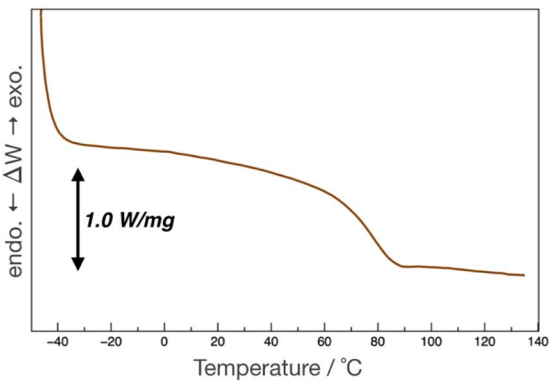


Fig. 3 DSC curve for the third heat scan of poly(dopamine acrylamide) (pDOPAm).

### Preparation of Janus metallic films by reduction of $AgNO_3$ using pDOPAm

Janus metallic films were prepared using pDOPAm as the reducing agent for $AgNO_3$. pDOPAm thin films with a thickness

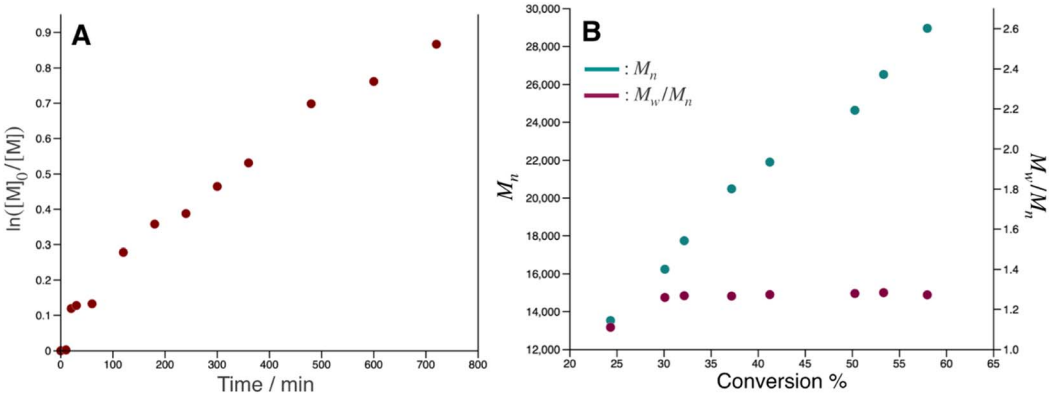


Fig. 1 (A) First-order kinetics of the reversible addition–fragmentation chain transfer polymerization of dopamine acrylamide. (B) Number-average molecular weight ($M_n$) and molecular weight dispersity ($M_w/M_n$) of poly(dopamine acrylamide) (pDOPAm) *vs.* the monomer conversion rate.

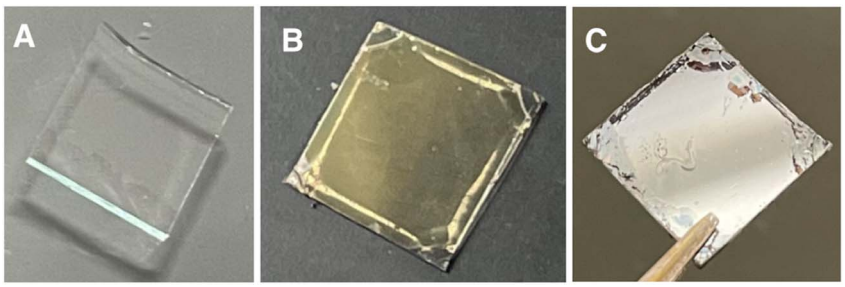


Fig. 4 Images of poly(dopamine acrylamide) (pDOPAm) thin films on glass substrates. Front side of the films after thermal annealing (A) under vacuum and (B) in aqueous $AgNO_3$ for 24 h. (C) Back side of the film shown in (B).

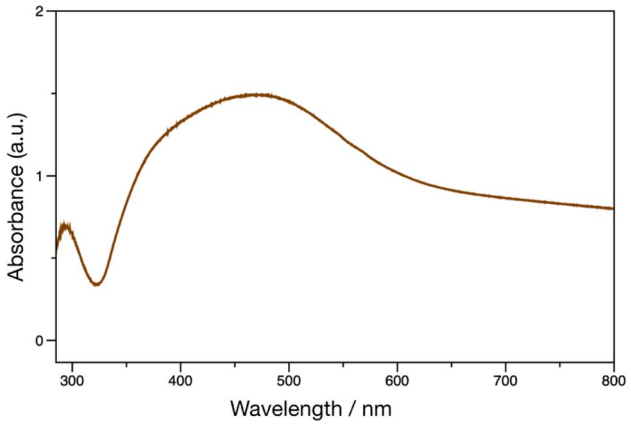


Fig. 5 UV-vis spectrum of Ag deposited on a poly(dopamine acrylamide) (pDOPAm) thin film. The electroless deposition of Ag was carried out at 80 °C for 24 h using aqueous $AgNO_3$.

of ~100 nm were spin-coated onto glass and quartz substrates. The pDOPAm-coated glass substrate was transparent (Fig. 4A). Subsequently, the films were immersed in aqueous $AgNO_3$ and thermally annealed at 80 °C for 24 h to deposit Ag *via* the reduction of silver ions (Fig. S3†). The color of the front side of the films (pDOPAm side) changed from transparent to gold after 24 h of reaction (Fig. 4B). On the other hand, the back side of the films (glass or quartz substrate side) exhibited a silver luster (Fig. 4C). Thus, Janus metallic films were successfully produced by the electroless deposition of silver using pDOPAm as the reductant. The UV-vis spectrum of the Janus metallic film on a quartz substrate revealed an absorption peak derived from the catechol group at 290 nm and a broad absorption peak extending from 340 to 600 nm, which was attributed to the plasmon resonance of Ag NPs (Fig. 5).[19] Thus, Ag NPs were formed on the pDOPAm thin film.

Subsequently, UV-vis reflectance measurements were performed to evaluate the reflectance colors on the front and back of the film. A dip in the reflectivity of the front side was observed at approximately 350–450 nm, which was similar to that of the Au foil (Fig. 6A). In contrast, the back side reflected most of the visible light above 400 nm, similar to the Ag plate (Fig. 6B). This difference in reflectivity resulted in the formation of a Janus metallic film.

### Coloration mechanism of the Janus metallic film

We performed SEM measurements to investigate the coloration mechanism of the Janus metallic film. The SEM images of the front (Fig. 7) and cross-section (Fig. 8) of the Janus metallic film show that Ag NPs with a diameter/length of 70–100 nm were formed throughout the film. Thus, the reflection of the incident light from the front occurred mainly because of the Ag NPs. The incident light above 400 nm was reflected because the Ag NPs were not uniform in size and shape and located close to each

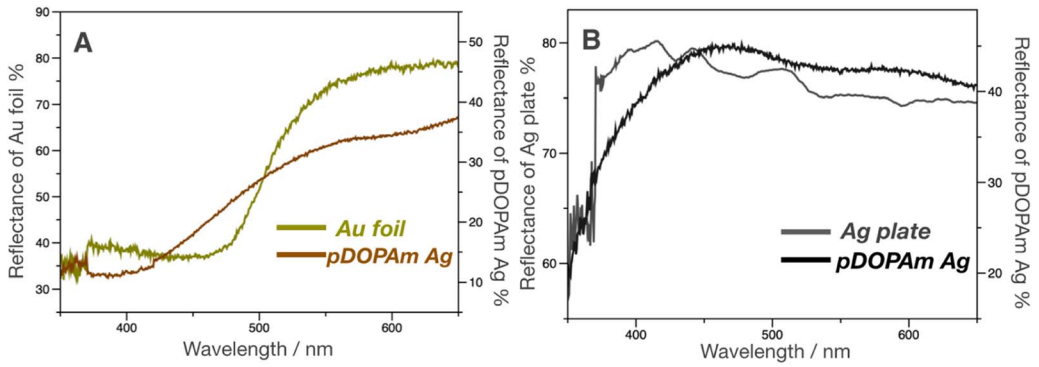


Fig. 6 Reflectance spectra of the (A) front (gold metallic luster) and (B) back sides (silver metallic luster) of a poly(dopamine acrylamide) (pDOPAm) thin film with deposited Ag. The reflectance spectra of an Au foil and Ag plate are presented as references. The electroless deposition of Ag was carried out at 80 °C for 24 h using aqueous $AgNO_3$.

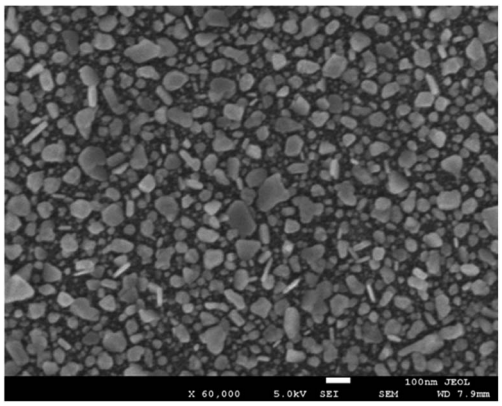


Fig. 7 SEM image of the front of a poly(dopamine acrylamide) (pDOPAm) thin film with electroless-deposited silver. Electroless deposition was performed at 80 °C for 24 h using aqueous $AgNO_3$.

other. The Ag NPs also exhibited light absorption. On the other hand, quinone, quinomethane, and their oligomer, which were produced by the oxidation of the catechol groups in the pDOPAm thin film, exhibited absorption below 510 nm,[20] which corresponds to the dip in the reflectance spectrum (Fig. 6A). Thus, a gold luster was observed on the front of the Janus metallic film owing to the combined visible-light absorption of oxidized pDOPAm and plasmon resonance (reflection and absorption) of the Ag NPs (Fig. 9A). On the other hand, the cross-sectional SEM images show the formation of a uniform Ag layer at the film–substrate interface. This Ag layer acted as a silver mirror, resulting in a silver luster on the back of the Janus metallic film (Fig. 9B).

Subsequently, we investigated the dependence of the metallic color on the duration of reaction between aqueous $AgNO_3$ and the pDOPAm thin film at 80 °C. The pDOPAm thin film was prepared on a Si substrate, and the color and surface

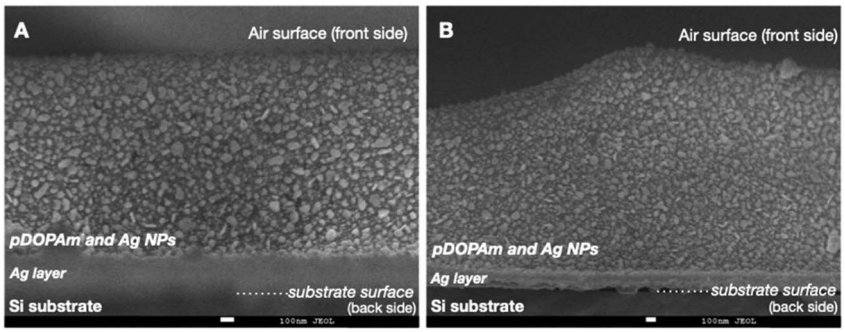


Fig. 8 Cross-sectional SEM images of a poly(dopamine acrylamide) (pDOPAm) thin film after electroless silver deposition ((A) magnification ×40 000 and (B) magnification ×30 000).

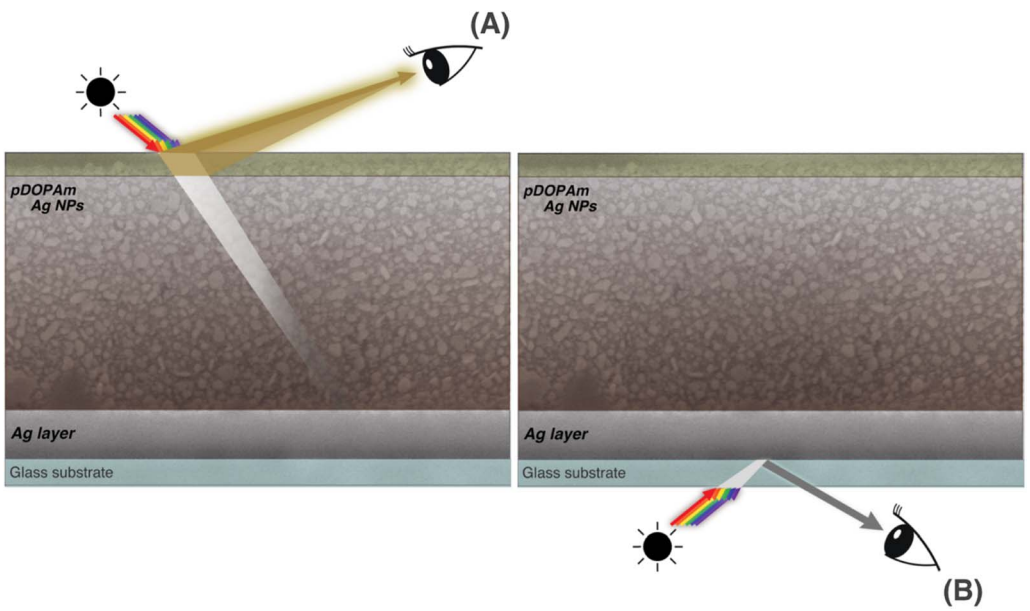


Fig. 9 Mechanism of Janus metallic coloration of a pDOPAm thin film. (A) On the front side, light is reflected from the surface and the Ag layer formed at the film–glass interface. Light reflected through the membrane is absorbed at 350–500 nm by the quinone form of catechol and Ag NPs. (B) On the back side, light is reflected by the Ag layer.

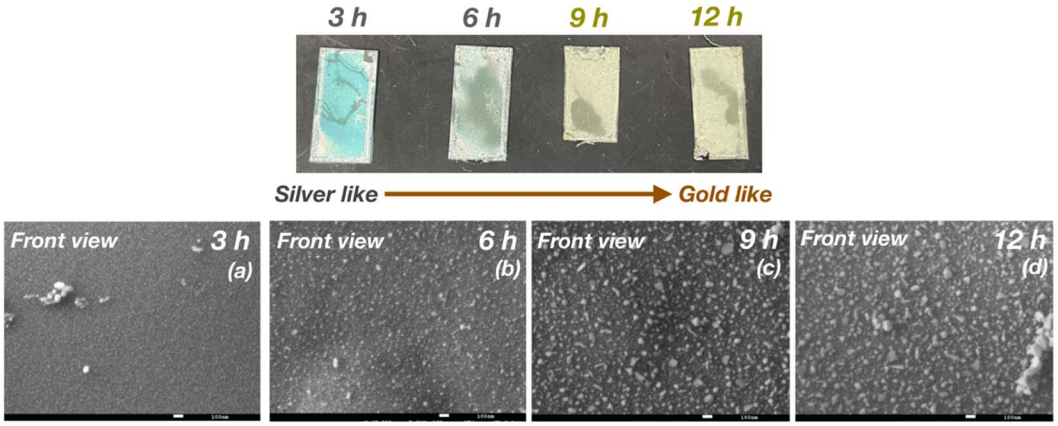


Fig. 10 Digital (top) and SEM images (bottom) of the front side of a poly(dopamine acrylamide) (pDOPAm) thin film after (a) 3, (b) 6, (c) 9, and (d) 12 h of electroless deposition of silver.

morphology of the front side were observed using a digital camera and scanning electron microscope, respectively (Fig. 10). The optical color of the film at 3–6 h of reaction was light blue to green, with a silver luster around the edge; however, a gold luster began to appear when the reaction time exceeded 12 h. The SEM images of the front side show that the amount of Ag NPs on the surface increased with increasing reaction time (Fig. 10 bottom). Cross-sectional SEM and EDS analyses were performed after 6 h (without gold luster) and 12 h (with gold luster). After 6 h, Ag was deposited mainly at the film–substrate interface and formed a silver mirror. After 12 h, the reacted film contained a silver layer and Ag NPs (Fig. 11). These results indicate that Ag deposition initially occurred mainly at the film/substrate interface, followed by the formation of Ag NPs inside the film. The polymer concentration at the spin-coated film–substrate interface is reportedly higher than that in the bulk.[21] Thus, the consumption of $Ag^+$ was faster at the film–substrate interface, creating a large concentration gradient in the vertical direction of the film and causing further accumulation of $Ag^+$ at the interface. Furthermore, as shown in the cross-sectional images, the film is highly swelled during the electroless deposition. However, the degree of swelling is considered to be low at the substrate interface because catechol groups strongly adhere to the substrate.[11] Therefore, the silver deposited close to the substrate/interface can connect each other to form a silver layer, whereas that at the bulk side forms particles because of the swelling of pDOPAm film.

The cyclic voltammogram of pDOPAm exhibited distinct 2-electron redox peaks with a formal potential of 137 mV *vs.* Ag/AgCl (Fig. S4†). This result is similar to a previously reported potential of catechol polymer (126 mV).[15] As the film was highly swelled during the electroless deposition, it is reasonable to presume that all pDOPAm were involved in the redox reaction. The catechol groups reduce silver ions to silver and change to benzoquinone (Scheme 2). The amount of catechol groups in 100 nm thick film with 1 $cm^2$ area was calculated to be 1.25 ×

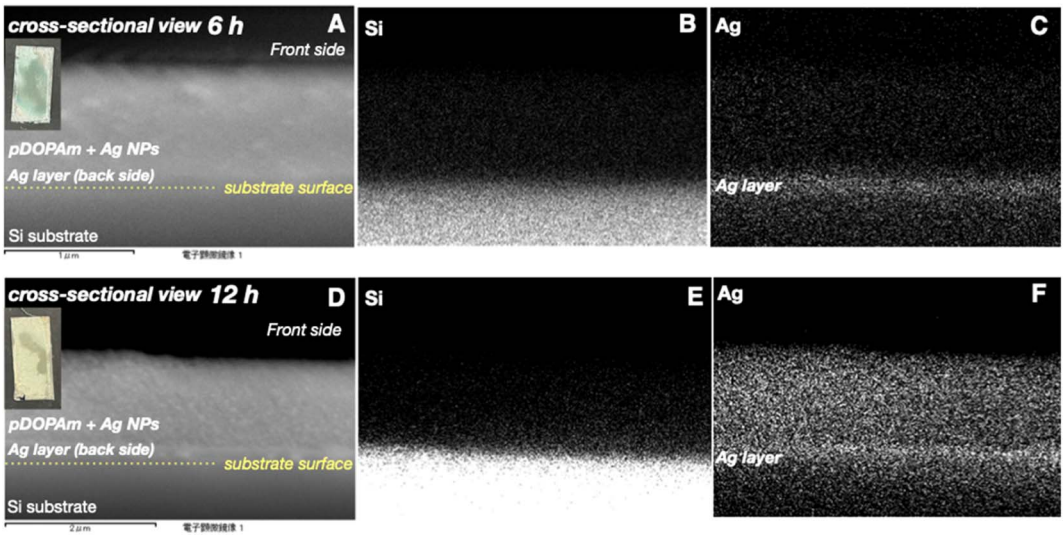


Fig. 11 (A, D) Cross-sectional SEM images of poly(dopamine acrylamide) (pDOPAm) and EDS mapping of (B, E) Si and (C, F) Ag after 6 (top) and 12 h (bottom) of electroless silver deposition.

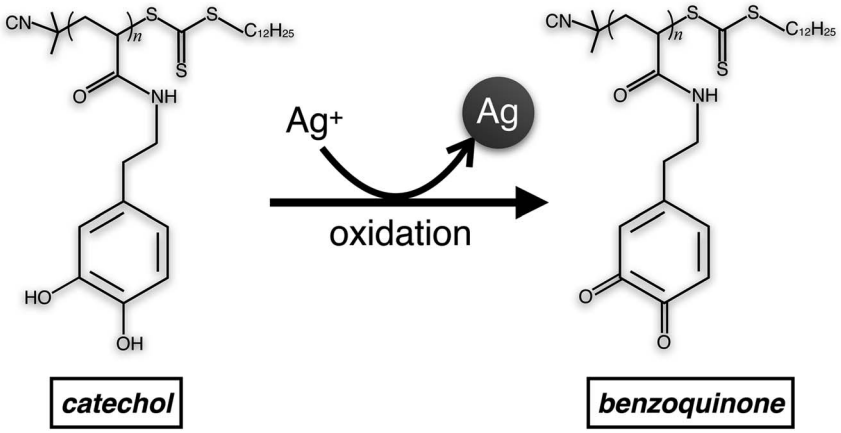


Scheme 2 The catechol groups reduce silver ions to silver and change to benzoquinone.

$10^{21}$, assuming the density of pDOPAm to 1.0 g $cm^{-3}$ based on the density of polystyrene (~1.0 g $cm^{-3}$). The number of silver atoms in a thickness of 1 μm (the swelled thickness) with a 1 $cm^2$ area was about 50 times higher ($5.86 \times 10^{22}$) than that of electrons produced by catechol groups. Because Ag NPs were formed and their density was not high, the amount of catechol groups was enough to produce the hybrid film.

A Janus metallic film was not formed when the reaction temperature was below 80 °C. The film was yellow at a reaction temperature of 20 °C and brown at 70 °C on either side (front or back; Fig. S5†). The reduction rate of $Ag^+$ was slow at low temperatures and a large concentration gradient was not formed. Therefore, a silver mirror was not produced at the film–substrate interface, and the film mainly exhibited the plasmon absorption of isolated (yellow at 20 °C) or aggregated (brown at 70 °C) Ag NPs. Notably, a silver luster on the front and back was only observed in a thick (more than 200 nm) pDOPAm film (Fig. S6†). This is because many Ag NPs were formed, and the incident light was mostly reflected from the front and back surfaces.

## Conclusion

A Janus metallic film with gold and silver luster at the front and back, respectively, was prepared using a pDOPAm thin film as a reducing agent for $Ag^+$. The gold luster was produced by the combined reflection of light by Ag NPs and absorption of oxidized pDOPAm and Ag NPs. In contrast, the silver luster was exhibited by the uniform silver layer at the film–substrate interface, whose formation was enabled by the high density of pDOPAm at the interface. Our method for creating Janus metallic films involves a simple one-pot process that generates a Au-like metallic luster using only Ag, unlike traditional methods, which require multiple steps. Furthermore, this study suggests that Janus metallic films can be widely applied as decorative and authentication materials.

## Author contributions

M. O. synthesized polymers, prepared Janus films measured SEM and wrote the first draft of the paper. R. A. analyzed the time conversion of the polymer, K. T. and M. K. measured and characterized the reflectance of the film. S. N. and H. E. characterized the optical properties of Janus film J. M. directed the whole project and wrote the final version of the manuscript.

## Conflicts of interest

The authors declare no conflict of interest.

## Acknowledgements

This work was supported by KAKENHI grant 22K18963 from the Japan Society for the Promotion of Science (JSPS), the JST, CREST grant number JPMJCR21B5, and the Research Program "Dynamic Alliance for Open Innovation Bridging Human, Environment and Materials" within the "Network Joint Research Center for Materials and Devices."

## References

1 J. W. Cho, E. J. Lee and S. K. Kim, *Nano Lett.*, 2022, **22**, 380–388.
2 A. K. Jahromi, S. Shabahang, H. E. Kondakci, S. Orsila, P. Melanen and A. F. Abouraddy, *ACS Photonics*, 2017, **4**, 1026–1032.
3 T. Shegai, S. Chen, V. D. Miljkovic, G. Zengin, P. Johansson and M. Kall, *Nat. Commun.*, 2011, **2**, 481.
4 K. Saito and T. Tatsuma, *ACS Photonics*, 2016, **3**, 1782–1786.
5 K. Saito and T. Tatsuma, *Adv. Opt. Mater.*, 2015, **3**, 883–887.
6 T. Kim, E. S. Yu, Y. G. Bae, J. Lee, I. S. Kim, S. Chung, S. Y. Lee and Y. S. Ryu, *Light Sci. Appl.*, 2020, **9**, 175.
7 N. R. Martinez Rodriguez, S. Das, Y. Kaufman, J. N. Israelachvili and J. H. Waite, *Biofouling*, 2015, **31**, 221–227.
8 J. H. Watte, *Integr. Comp. Biol.*, 2002, **42**, 1172–1180.
9 H. Lee, N. F. Scherer and P. B. Messersmith, *Proc. Natl. Acad. Sci. U.S.A.*, 2006, **103**, 12999–13003.
10 J. Yu, Y. Kan, M. Rapp, E. Danner, W. Wei, S. Das, D. R. Miller, Y. Chen, J. H. Waite and J. N. Israelachvili, *Proc. Natl. Acad. Sci. U.S.A.*, 2013, **110**, 15680–15685.

11 H. Lee, S. M. Dellatore, W. M. Miller and P. B. Messersmith, *Science*, 2007, **318**, 426–430.
12 H. Komiyama, D. Hojo, K. Z. Suzuki, S. Mizukami, T. Adschiri and H. Yabu, *ACS Appl. Nano Mater.*, 2018, **1**, 1666–1674.
13 L. Zhang, Z. Liu, Y. Wang, R. Xie, X.-J. Ju, W. Wang, L.-G. Lin and L.-Y. Chu, *Chem. Eng. J.*, 2017, **309**, 691–699.
14 S. Ma, L. Liu, V. Bromberg and T. J. Singler, *J. Mater. Chem. C*, 2014, **2**, 3885–3889.
15 E. Grignon, S. Y. An, A. M. Battaglia and D. S. Seferos, *Macromolecules*, 2022, **55**, 10167–10175.
16 N. Jiménez, F. Ruipérez, E. González de San Román, J. M. Asua and N. Ballard, *Macromolecules*, 2021, **55**, 49–64.
17 N. Patil, C. Falentin-Daudré, C. Jérôme and C. Detrembleur, *Polym. Chem.*, 2015, **6**, 2919–2933.
18 L. A. Burzio and J. H. Waite, *Biochem.*, 2000, **39**, 11147–11153.
19 G. Merga, R. Wilson, G. Lynn, B. H. Milosavljevic and D. Meisel, *J. Phys. Chem. C*, 2007, **111**, 12220–12226.
20 S. Takahashi, K. Kishikawa and M. Kohri, *Polym. J.*, 2022, **54**, 1039–1043.
21 Y. Jiang, M. Minett, E. Hazen, W. Wang, C. Alvarez, J. Griffin, N. Jiang and W. Chen, *Langmuir*, 2022, **38**, 12702–12710.